JOURNAL OF SOLID STATE CHEMISTRY 39, 298–308 (1981)

Mechanism of Ni–Zn Ferrite Formation

V. V. PAN'KOV AND L. A. BASHKIROV

Institute of Solid State Physics and Semiconductors, Byelorussian Academy Of Sciences, Minsk, Podlesnaya 17, 220726 USSR

Received June 20, 1980; in revised form April 30, 1981

The regularities in the change of character of the ferrite formation process as a function of $Ni_{1-x}Zn_xFe_2O_4$ solid solution and of the degree of zinc oxide saturation of the $Ni_{1-x}Zn_xO$ solid solution ($x = 0.14; 0.29; 0.43$) are established in the temperature range 1220–1305°C. It is shown that in the reaction zone of interacting NiO, (Ni, ZnO), or ZnO with Fe_2O_3 the ferrite phase crystallizes only on iron oxide. The distribution of the Fe, Ni, and Zn concentrations over the reaction layer thickness using electron probe and X-ray spectrum analysis is obtained. The interdiffusion coefficients over the investigated temperature range calculated in the (Ni, Zn, Fe)O and ferrite phases change from $(0.8 - 7.0) \times 10^{-9}$ to $(1.0 - 12.0) \times 10^{-10}$ cm²/sec, respectively. The interaction of (Ni, Zn)O with Fe_2O_3 takes place by the mechanism of interaction of interdiffusion of Fe^{3+}, Fe^{2+} and Ni^{2+}, Zn^{2+} along with a current of Zn^{2+} ions and electrons or oxygen ions directed to the ferrite/Fe_2O_3 interface.

Introduction

In preparing Ni–Zn ferrites by the ceramic method from the oxide mixtures of NiO, ZnO, Fe_2O_3 the ferrite formation process is carried out by a series of intermediate solid solution transformations (*1*). One of these stages is the interaction between the (Ni, Zn)O solid solution and iron oxide, formed as a result of direct interaction of NiO with ZnO as well as by the reaction of $ZnFe_2O_4 + NiO \rightarrow (Ni, Zn)Fe_2O_4 + (Ni, Zn)O$ (*2*). Sometimes the Ni–Zn ferrites synthesis is carried out by the annealing of $NiCO_3$ ZnO, Fe_2O_3 mixtures. However, the nickel carbonate decomposition in them precedes the ferrite formation process (*3*). It is possible that in this case as well one of the Ni–Zn ferrite synthesis stages is the interaction of Fe_2O_3 with solid solution (Ni, Zn)O, the formation of which due to higher activity of NiO can proceed at a higher rate than that in the mixtures of the initial oxides NiO, ZnO, Fe_2O_3. While studying this reaction for the (Ni, Zn)O solid solution with different zinc quantities one can see the change of the ferrite formation mechanism on passing from nickel ferrite to zinc ferrite. With this aim in view the interaction of the coagulated pellets of Fe_2O_3 with NiO, ZnO pellets and (Ni, Zn)O solid solutions, containing 14, 29, and 43 mole% of ZnO are investigated in this paper.

Experimental

The (Ni, Zn)O solid solution powders were obtained by the coprecipitation method. These powders as well as those of NiO, ZnO, and Fe_2O_3 were pressed under pressure of 1.5×10^2 MPa into pellets (10 mm in diameter and 5–6 mm in height). The annealing of the pellets was carried out in

0022-4596/81/120298-11$02.00/0

Copyright © 1981 by Academic Press, Inc.
All rights of reproduction in any form reserved.

air at 1250°C for 24 hr with subsequent quenching. The $Ni_{0.57}Zn_{0.43}O$ solid solution was additionally annealed at 1400°C for 7 hr. A series of experiments was carried out on the NiO single-crystal plates (0.1 cm thick) cleaved along the (100) plane from the single crystal grown by the Verneuil method.

The diffusion annealings of the pellet couples were carried out in air at 1215, 1240, 1265, 1295, 1305, and 1325°C. During the annealing the contact between the polished pellet surfaces was made constant by a special device. To find the initial interface, a thin platinum line was precipitated on the Fe_2O_3 pellet or a platinum wire (30 μm in diameter) was laid on the surface. The reaction layer between the interacting pellets was studied by microstructure, X-ray phase, and electron probe X-ray spectrum analyses. The variation of Ni, Zn, and Fe content with reaction zone thickness was determined by an X-ray microanalyser "MS-46." The electron beam traveled continuously on the section surface. The intensity of characteristic irradiation was determined for two elements at each point simultaneously. The composition of the section range far removed from the reaction zone corresponding to that of the initial pellet interface was used as a standard for converting the element irradiation intensity to concentration.

Results

Figure 1 shows the microstructure and the appearance of the reaction zones of the Fe_2O_3, (Ni, Zn)O, NiO pellets in the systems of (a) NiO (single crystal)–Fe_2O_3, (b) $Ni_{0.86}Zn_{0.14}O$–Fe_2O_3. (c) $Ni_{0.71}Zn_{0.29}O$–Fe_2O_3, (d) $Ni_{0.57}Zn_{0.43}O$–Fe_2O_3. Distribution of the Ni, Zn, Fe concentration over the zone thickness for the $Ni_{0.57}Zn_{0.43}O$–Fe_2O_3 system is given in Fig. 2. The change in character of these curves in general, is also preserved for the systems with other concentrations of the (Ni, Zn)O solid solution at different temperatures of annealing. The reaction zone of the solid phase interaction of NiO or (Ni, Zn)O with Fe_2O_3 is found to consist of the diffusion layer of the (Ni, Fe)O or (Ni, Zn, Fe)O solid solutions and the layer of the ferrite phase. The solid solution layer (Ni, Fe)O or (Ni, Zn, Fe)O is located essentially on the NiO and (Ni,

TABLE I

THE ANNEALING REGIME AND NUMBERING OF THE LAYERS IN FIG. 1

Fig.	System	Annealing regime		Reaction zone layers			
		Time (hr)	Temperature (°C)	Fe_2O_3	(Ni, Fe)Fe_2O_4, (Ni, Zn, Fe)Fe_2O_4 on the Fe_2O_3 pellet	(Ni, Fe)O (Ni, Zn, Fe)O on the Fe_2O_3 pellet	(Ni, Fe)O (Ni, Zn, Fe)O on the NiO single crystal (Ni, Zn)O pellet
1a	NiO–Fe_2O_3 single crystal	87	1305	1	2	3	4
1b	$Ni_{0.86}Zn_{0.14}O$–Fe_2O_3	77	1265	1	2	3	—
1c	$Ni_{0.71}Zn_{0.29}O$–Fe_2O_3	51	1265	1	2	3	—
1d	$Ni_{0.57}Zn_{0.43}O$–Fe_2O_3	99	1265	1	2	3	4

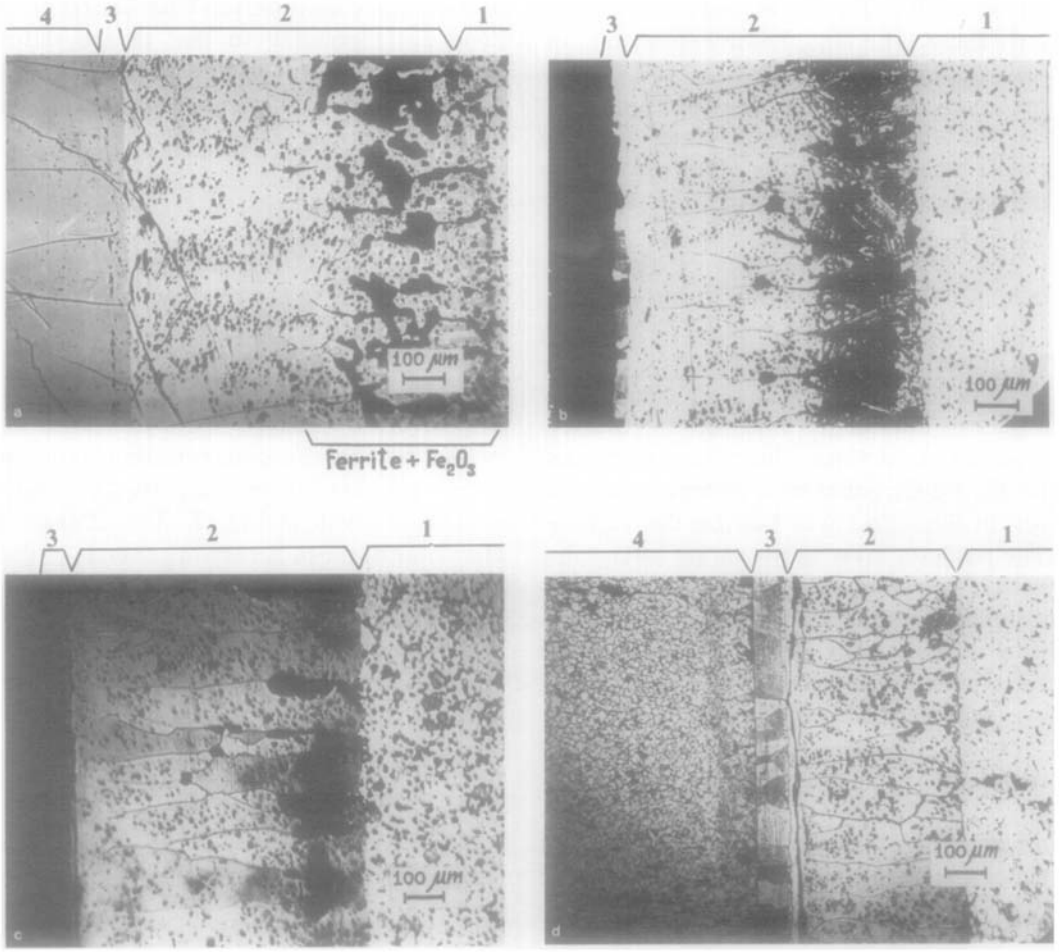

FIG. 1. Microstructure of the reaction zones of the diffusion couples NiO (single crystal)–Fe_2O_3 (a); $Ni_{0.86}Zn_{0.14}O$–Fe_2O_3 (b); $Ni_{0.71}Zn_{0.29}O$–Fe_2O_3 (c); $Ni_{0.57}Zn_{0.43}$–Fe_2O_3 (d). The annealing regime and numbering of the layers are given in Table I.

Zn)O pellets (Figs. 1, 2, layer 4) and partially on Fe_2O_3 (layer 3). The ferrite phase is formed only on the Fe_2O_3 pellet (layer 2).

For all the compositions the growth kinetics of the (Ni, Zn, Fe)O layer on the (Ni, Zn)O pellets (Fig. 3a) and that of the ferrite layer on the Fe_2O_3 pellets (Fig. 3b) are described by the equation $x^2 = kt$. In the case of the (Ni, Zn, Fe)O layer, the parabolic constant k for the interaction of Fe_2O_3 with NiO, $Ni_{0.86}Zn_{0.14}O$, $Ni_{0.71}Zn_{0.29}O$, $Ni_{0.57}Zn_{0.43}$, and ZnO at 1265°C is 1.5×10^{-8}; 2.6×10^{-8}; 3.3×10^{-8}; 5.3×10^{-8}, and 0.7×10^{-8} cm²/sec, respectively. For the ferrite layer at the same temperature it is about an order of magnitude less and is 5.7×10^{-9}; 6.3×10^{-9}; 7.5×10^{-9}; 7.9×10^{-9}; 11.5×10^{-9} cm²/sec. In the investigated temperature range the parabolic constant k varies in accordance with the Arrhenius equation $k = k_0 \exp(-Q/RT)$. In this case the values of the activation energy and those of the exponential factor for the kinetic growth constant k of the ferrite layer decreases in the series NiO–Fe_2O_3; (Ni, Zn)O; ZnO-Fe_2O_3. The activation energy of

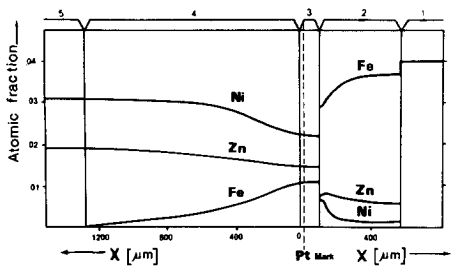

FIG. 2. The distribution of the Fe, Ni, Zn concentrations over the reaction zone thickness of the diffusion couple $Ni_{0.57}Zn_{0.43}O$–Fe_2O_3 annealed at 1265°C for 110.3 hr. The Fe_2O_3 pellet: layers Fe_2O_3 (1); (Ni, Zn, Fe) Fe_2O_4 (2); (Ni, Zn, Fe)O (3); The $Ni_{0.57}Zn_{0.43}O$ pellet: layers (Ni, Zn, Fe)O (4); $Ni_{0.57}Zn_{0.43}O$ (5); (----) initial interface of two pellets.

the ferrite layer growth is much greater than that of the (Ni, Zn, Fe)O layer (Table II). Two layers (Fig. 1 layers 2, 3) are clearly seen with the microscope on the Fe_2O_3 pellet. On the Fe_2O_3 pellet a smaller diffusion layer (layer 3) immediately adjoining the diffusion layer of the (Ni, Zn)O or NiO pellet is found to be also the (Ni, Zn, Fe)O, (Ni, Fe)O solid solution and its composition changes negligibly with thickness. This layer is more dense in comparison with the diffusion layer on the (Ni, Zn)O pellet. With large magnification dendrites, probably of the ferrite phase, deposited during oxidation in cooling the (Ni, Zn, Fe)O solid solution (Fig. 4, layer 3) are observed. The fact that this layer on the Fe_2O_3 pellet belongs to the (Ni, Zn, Fe)O phase rather than to the ferrite phase is also proved by the magnetic suspension deposited on the specimen section. When a magnetic field is applied, an even band appears on the inner interface of the first diffusion layer of the Fe_2O_3 pellet (Fig. 5a,b) showing the (Ni, Zn, Fe)O layer to be magnetic. The (Ni, Zn, Fe)O layer size on the Fe_2O_3 pellet for the investigated systems under the same thermal treatment conditions grows with the Zn concentration in the (Ni, Zn)O solid solutions. For the ZnO–Fe_2O_3 system this layer has not been detected.

At the (Ni, Zn, Fe)O/ferrite interface, the iron concentration in (Ni, Zn, Fe)O is equal to the solubility limit of iron oxides in (Ni, Zn)O or NiO, which are in equilibrium with the Ni–Zn ferrite solid solutions. In the investigated temperature range the solubility of iron oxides in NiO and (Ni, Zn)O changes slightly, however, a tendency to decrease is observed with decreasing temperature (Table III). There is no great difference between the iron oxide solubility in NiO and that of (Ni, Zn)O. The oriented crystal growth along the diffusion direction is found in the Ni–Zn ferrite layer only on the Fe_2O_3 pellet (Fig. 1b,c,d). The texture is also revealed on X-ray diffraction patterns taken from the Fe_2O_3 pellets reaction layer surface. The intensity of the (220), (222), (440) reflections on them is higher and that

TABLE II

TEMPERATURE-DEPENDENCE PARAMETERS OF THE RATE CONSTANTS OF (Ni, Fe, Zn)O AND FERRITE LAYER GROWTH

System	Ferrite layer		(Ni, Zn, Fe)O layer	
	Q (kcal/mole)	k_0 (cm²/sec)	Q (kcal/mole)	k_0 (cm²/sec)
NiO–Fe_2O_3	121.6 ± 0.4	1.4×10^9	58.9 ± 4.9	2.8
$Ni_{0.86}Zn_{0.14}$–Fe_2O_3	120.5 ± 2.0	9.1×10^8	69.1 ± 4.3	1.9×10^2
$Ni_{0.71}Zn_{0.29}O$–Fe_2O_3	105.1 ± 6.0	7.0×10^6	57.1 ± 4.5	4.3
$Ni_{0.57}Zn_{0.43}O$–Fe_2O_3	106.5 ± 9.0	1.2×10^7	65.9 ± 3.9	85
ZnO–Fe_2O_3	98.1 ± 5.7	1.1×10^6	62.8 ± 3.0	5.7

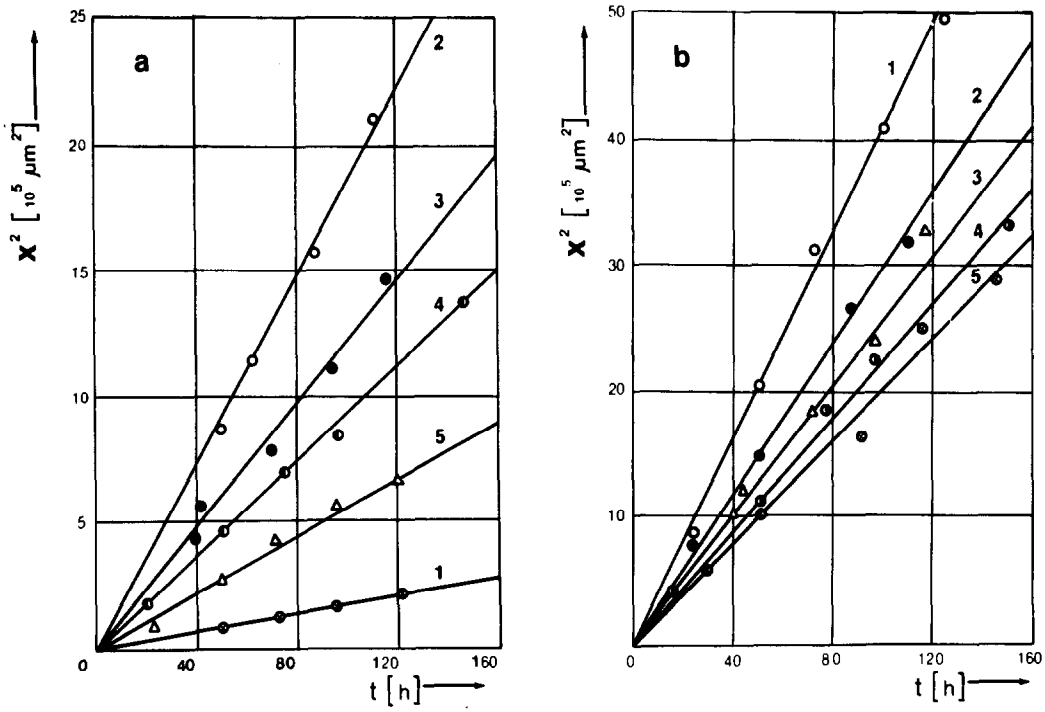

FIG. 3. Thickness squared of the layer (x^2) vs time of annealing (t) at 1265°C for the diffusion couples: ZnO–Fe_2O_3 (1) $Ni_{0.57}Zn_{0.43}O$–Fe_2O_3 (2); $Ni_{0.71}Zn_{0.29}O$–Fe_2O_3 (3); $Ni_{0.86}Zn_{0.14}O$–Fe_2O_3 (4); NiO–Fe_2O_3 (5). For the (Ni, Zn, Fe)O layer on the (Ni, Zn)O pellet (a), for the ferrite layer (b).

of (311) and others is lower than those on the X-ray diffraction patterns of ferrite powders of the corresponding composition. In the ferrite layer at the boundary with Fe_2O_3 there is an accumulation of pores elongated towards the interface with (Ni, Zn, Fe)O (Fig. 1a,b,c). The quantity of pores is noted to decrease with zinc content increasing in the (Ni, Zn)O solid solution. The most probable reason for their formation is the accumulation of cation vacancies diffusing from the inner reaction layer to the phase boundary ferrite/Fe_2O_3. But it is probable that its appearance is caused by the volume decrease of the Fe_2O_3 pellet reaction zone due to the Fe_2O_3 dissociation to magnetite and substitution of the Fe^{2+} ions of magnetite by the Ni^{2+}, Zn^{2+} ions (*4*). For zinc ferrite and nickel ferrite this decrease equals 1.0% and 4.6%, respectively.

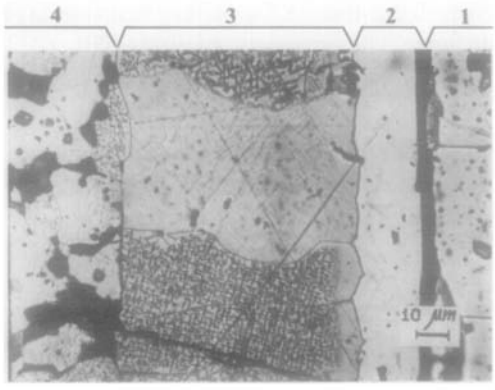

FIG. 4. Microstructure of the reaction layer area of the diffusion couple $Ni_{0.57}Zn_{0.43}O$–Fe_2O_3 annealed for 99 hr at 1240°C. (1) (Ni, Zn, Fe) Fe_2O_4; (2) (Ni, Zn) Fe_2O_4; (3) the dense layer (Ni, Zn, Fe)O on the Fe_2O_3 pellet; (4) (Ni, Zn, Fe)O on the (Ni, Zn, Fe)O pellet.

In all the investigated systems variation of the ferrite phase composition over the reaction layer thickness (Fig. 2, layer 2) is observed. On passing from the phase boundary (Ni, Zn, Fe)O/ferrite to the ferrite/Fe_2O_3 boundary the iron content

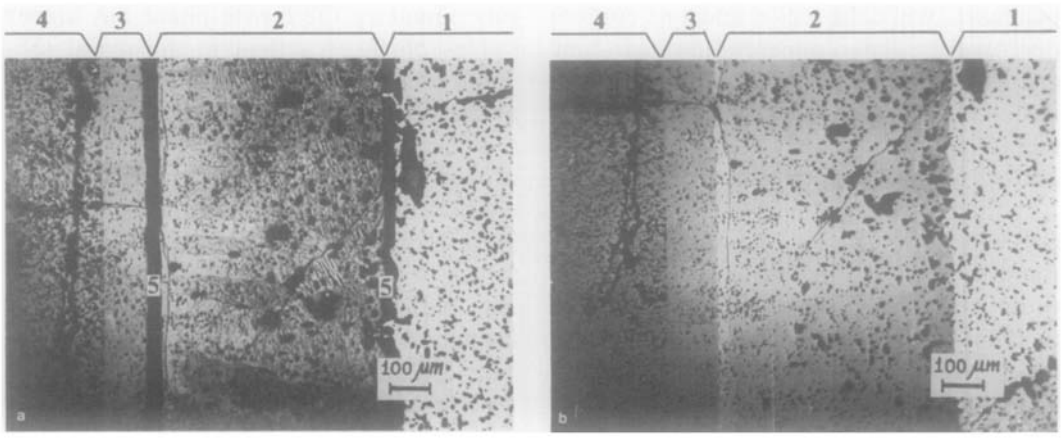

FIG. 5. Reaction zone of the diffusion couple $Ni_{0.57}Zn_{0.43}O$–Fe_2O_3 annealed at 1265°C for 110.3 hr. The Fe_2O_3 layer (1), (Ni, Fe, Zn) Fe_2O_4 (2); the (Ni, Zn, Fe)O layer on the Fe_2O_3 pellet (3); the (Ni, Zn, Fe)O layer on the $Ni_{0.47}Zn_{0.43}O$ pellet (4); the magnetic suspension line (5). Zone area (a) with magnetic suspension, and (b) without it.

TABLE III

PHASE COMPOSITIONS AT INTERFACES IN THE (Ni, Zn)O–Fe_2O_3 SYSTEMS

Pellet composition (Ni, Zn)O	Annealing temp. (°C)	Ferrite composition at the boundary with Fe_2O_3 atomic fractions			Ferrite composition at the boundary with (Ni, Zn, Fe)O atomic fractions			(Ni, Zn, Fe)O composition at the boundary with ferrite atomic fractions		
		C_{Fe}	C_{Ni}	C_{Zn}	C_{Fe}	C_{Ni}	C_{Zn}	C_{Fe}	C_{Ni}	C_{Zn}
NiO	1325	0.385	0.045	—	0.315	0.155	—	0.110	0.415	—
single crystal	1305	0.370	0.045	—	0.320	0.150	—	0.110	0.395	—
	1265	0.380	0.045	—	0.320	0.125	—	0.100	0.420	—
$Ni_{0.86}Zn_{0.14}O$	1295	0.355	0.050	0.035	0.315	0.085	0.030	0.085	0.350	0.055
	1265	0.350	0.050	0.030	0.295	0.120	0.040	0.085	0.335	0.055
	1240	0.342	0.075	0.035	0.305	0.125	0.040	0.070	0.370	0.040
	1215	0.333	0.060	0.035	0.290	0.085	0.045	0.085	0.355	0.050
$Ni_{0.71}Zn_{0.29}O$	1295	0.365	0.025	0.045	0.275	0.100	0.075	0.095	0.295	0.095
	1265	0.355	0.025	0.055	0.300	0.095	0.075	0.085	0.330	0.130
	1240	0.345	0.025	0.050	0.290	0.050	0.065	0.085	—	—
	1215	0.340	0.025	0.085	0.295	0.100	0.095	0.080	—	—
$Ni_{0.57}Zn_{0.43}O$	1295	0.365	0.010	0.050	0.275	0.065	0.070	0.100	0.230	0.165
	1265	0.360	0.010	0.055	0.285	0.080	0.080	0.110	0.215	0.145
	1240	0.355	0.010	0.070	0.290	0.045	0.085	0.110	0.245	0.170
	1215	0.345	0.010	0.075	0.285	0.050	0.085	0.095	0.230	0.180
ZnO	1295	0.370	—	0.065	0.290	—	0.145	—	—	—
	1265	0.365	—	0.105	0.290	—	0.175	—	—	—
	1215	0.360	—	0.060	0.315	—	0.100	—	—	—

increases, while the nickel and zinc content decreases. The concentration of zinc changes less than that of nickel in the layer thickness. The concentration of these elements changes mostly near the phase boundary (Ni, Zn, Fe)O/ferrite.

In the ferrite layer near the phase boundary with (Ni, Zn, Fe)O a small range is found where the iron concentration is close to its stoichiometric value in ferrite, equal to 0.286 atomic fraction (Table III). This range is clearly seen on the sections annealed additionally in air at 800°C (Fig. 6). In this case the microstructure changes of the whole section connected with the oxidation of the Fe^{2+} ions of the ferrite layer take place with the exception of the narrow band at the (Ni, Zn, Fe)O/ferrite phase boundary. In this reaction layer range there is observed a higher value of the C_{Zn}/C_{Ni} ratio than that in the initial (Ni, Zn)O solid solution, which agrees with (*5*) and with the $NiO–ZnO–Fe_2O_3$ phase diagram (*6*). At the phase boundary with Fe_2O_3, the iron atomic fraction in the ferrite is 0.331–0.385 (Table III), which is much higher than that in the ferrite with stoichiometric composition and smaller than that (0.429) for magnetite. At this boundary the ferrite phase has higher values of C_{Zn}/C_{Ni} than in the initial (Ni, Zn)O solid solution and in the ferrite phase at the boundary (Ni, Zn, Fe)O/ferrite.

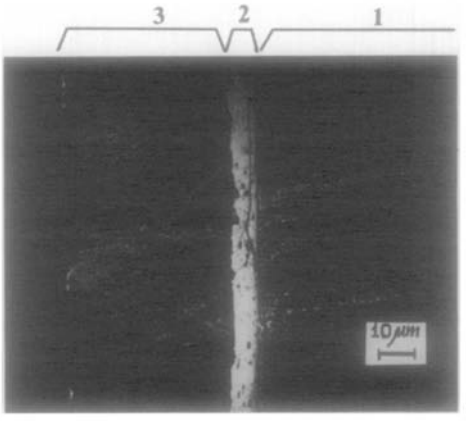

FIG. 6. Reaction zone of the additionally annealed at 800°C Fe_2O_3 pellet of the diffusion couple in air $Ni_{0.57}Zn_{0.43}O–Fe_2O_3$ (the temperature of diffusion annealing is 1295°C). Layers (Ni, Zn, Fe) Fe_2O_4 (1), (Ni, Zn) Fe_2O_4 (2), (Ni, Zn, Fe)O (3).

The coefficients of cation interdiffusion are determined by the Boltzmann–Matano method using the iron distribution curves both in the (Ni, Zn, Fe)O layer and in the ferrite layer near the phase boundary (Ni, Zn, Fe)/O/ferrite, where the greatest change of iron concentration is observed. The Matano plane, dividing the overall iron flow into two equal parts, is determined from the expression given in (*7*). For a majority of diffusion paris the Matano plane is located near the initial interface in the (Ni, Zn, Fe)O solid solution layer on the Fe_2O_3 pellet. Over the temperature range 1215–1295°C the interdiffusion coefficient $\tilde{D}$ in the (Ni, Zn, Fe)O phase varies from 0.8×10^{-9} to 7.0×10^{-9} cm²/sec. Depending on the iron concentration C_{Fe}, it varies within this range. With atomic fraction C_{Fe} ranging from 0.075 to 0.035, the activation energy of cations interdiffusion decreases by 15–30 kcal/mole (Table IV).

In the ferrite phase the $\tilde{D}$ values are approximately an order of magnitude smaller than those in the (Ni, Zn, Fe)O phase. For $C_{Fe} = 0.31$ atomic fraction the interdiffusion coefficient in the $\tilde{D}$ ferrite phase of the investigated systems ranges from 1×10^{-10} to 12×10^{-10} cm²/sec. The increase of zinc content in the initial solid solution (Ni, Zn)O leads within this order to increase of the interdiffusion coefficient in the phases (Ni, Zn, Fe)O and (Ni, Zn, Fe) Fe_2O_4 and to decrease of the activation energy (Table IV), i.e., to increasing rate of interaction of Fe_2O_3 with (Ni, Zn)O. The obtained interdiffusion coefficients make it possible to account for the formation of the (Ni, Zn, Fe)O solid solution layer on the Fe_2O_3 particles. In interacting (Ni, Zn)O with Fe_2O_3 the interdiffusion coefficient in the (Ni, Zn, Fe)O phase is an order of magnitude larger than that in the ferrite

TABLE IV

ACTIVATION ENERGY Q AND PREEXPONENTIAL MULTIPLIER $\tilde{D}_0$ OF THE INTERDIFFUSION COEFFICIENTS FOR THE (Ni, Zn, Fe)O LAYER

Fe content in (Ni, Zn, Fe)O (atomic fraction)	$Ni_{0,57}Zn_{0,43}O$–Fe_2O_3		$Ni_{0,71}Zn_{0,29}O$–Fe_2O_3		$Ni_{0,86}Zn_{0,14}O$–Fe_2O_3	
	Q (kcal/mole)	$\tilde{D}_0$ (cm^2/sec)	Q (kcal/mole)	$\tilde{D}_0$ (cm^2/sec)	Q (kcal/mole)	$\tilde{D}_0$ (cm^2/sec)
0.075	71 ± 11	5.5×10^{1}	79 ± 11	5.2×10^{2}	86 ± 15	4.0×10^{3}
0.055	57 ± 11	4.9×10^{-1}	69 ± 7	1.7×10^{1}	71 ± 16	2.6×10^{1}
0.035	50 ± 4	5.6×10^{-2}	62 ± 5	2.0	53 ± 5	6.8×10^{-2}

phase, and the iron diffusion through the ferrite layer limits the process as a whole. As a result, the quantity of iron ions going to the phase boundary (Ni, Zn, Fe)O/ferrite is smaller than that going into the (Ni, Zn)O particle or NiO. Then in some part of the ferrite layer near the boundary with (Ni, Zn, Fe)O the iron concentration decreases so that its structure becomes unstable and transforms into the (Ni, Zn, Fe)O solid solution structure. This phase transformation is not observed in zinc ferrite formation due to low solubility of iron oxides in zinc oxide.

For all the systems except that of NiO–Fe_2O_3 it is found that the ferrite layer on the Fe_2O_3 pellet edge bends and stretches out along the side surface, gradually reducing its thickness. The X-ray spectrum analysis data show that this ferrite layer range has higher zinc concentration. The higher the zinc concentration in (Ni, Zn)O, the greater is the length of the bend, reaching a maximum for the diffusion pairs of the ZnO–Fe_2O_3 system. These experimental data indicate the possibility of ZnO transport through the gaseous phase. To confirm the transport of Zn, annealings of the NiO–Fe_2O_3; (Ni, Zn)O–Fe_2O_3; ZnO–Fe_2O_3 diffusion couples were carried out at 1295 and 1240°C, where a platinum plate (0.2 mm thick) with an aperture (1 mm in diameter) in the center was placed between the reagent pellets. The formation of the reaction layer in the gap between the pellets is established in all the systems, with the exception of the NiO–Fe_2O_3 diffusion couple, only on the Fe_2O_3 pellets. This layer is found to be a solid solution of zinc ferrite and magnetite. No nickel has been found in it indicating that there is no nickel transfer through the gaseous phase. The larger the ferrite layer value, the higher is the zinc concentration in the initial (Ni, Zn)O solid solution and it is a maximum for the ZnO–Fe_2O_3 diffusion pair.

Discussion

From the present studies it follows that as a result of interaction of (Ni, Zn)O solid solution with Fe_2O_3, the formation of Ni–Zn ferrite takes place essentially by the mechanism of Fe^{3+}, Fe^{2+} and Ni^{2+}, Zn^{2+} ion interdiffusion, with the ferrite crystallizing only on the Fe_2O_3 particles. In this case the iron ion diffusion in (Ni, Zn)O results in formation of only the (Ni, Zn, Fe)O solid solution in which the iron concentration does not reach a value high enough for ferrite phase crystallization to occur. In this case, by using this mechanism two extreme cases are possible.

The first case is analogous to the Wagner model, where the Fe^{3+}, Ni^{2+}, and Zn^{2+} ions diffuse through the formed layer of the ferrite phase. At the phase boundaries of ferrite/Fe_2O_3 and (Ni, Zn, Fe)O/ferrite the

reactions proceed accordingly:

$$4\,Fe_2O_3 + 3(Ni^{2+}, Zn^{2+}) = 3(Ni, Zn)Fe_2O_4 + 2\,Fe^{3+}$$

$$n(Ni, Zn)O + 2\,Fe^{3+} = n(Ni, Zn, Fe)O + 3\,(Ni^{2+}, Zn^{2+})$$

For this case the equivalent volume of the forming ferrite phase is $3/6V_M$, where V_M is the molar volume of (Ni, Zn) Fe_2O_4 and the reaction rate rational constant K_r is determined by the Wagner–Schmalzried expression (*8*):

$$K_r = Z_c\, C_c \tilde{D}_c \frac{4}{3} \frac{\Delta G^0}{RT}$$

where Z_c, C_c, and $\tilde{D}_c$ are charge, concentration in equivalent volume units, and the diffusion cation coefficient limiting the reaction rate, respectively: ΔG^0 is the free energy of the ferrite formation from the oxides. According to the model of the first extreme case the iron transfer is carried out only by the Fe^{3+} ions and the forming ferrite should not contain Fe^{2+}. However, as evidenced by the obtained experimental data, the ferrite phase forming at the boundary with Fe_2O_3 contains a considerable amount of dissolved magnetite. Consequently, it should be assumed that in these reactions the iron transfer is carried out not only by the Fe^{3+} ions, but also by the Fe^{2+} ions.

The case when the iron transport is carried out only by the Fe^{2+} ions (the second extreme case of the interdiffusion mechanism under study) corresponds to the model proposed in (*4*), accounting for the mechanism of interaction between NiO and Fe_2O_3. According to this model, nickel ferrite crystallizes at the phase boundary Fe_2O_3/ferrite as a result of partial substitution of the Fe^{2+} ions of magnetite, formed by reaction of ferric oxide thermal decomposition $3\,Fe_2O_3 = 2\,Fe_3O_4 + \frac{1}{2}\,O_2$, by the Ni ions of NiO. Hence, in the investigated systems the Ni–Zn solid solution of ferrite with magnetite at the phase boundary of the reaction layer with Fe_2O_3 forms also by the reaction:

$$3Fe_2O_3 + 2(1-x)(Ni^{2+}, Zn^{2+}) = 2(Ni, Zn)_{1-x}Fe_{2+x}O_4 + 2(1-x)Fe^{2+} + \tfrac{1}{2}O_2.$$

On the other side of the ferrite layer, at the boundary with (Ni, Zn, Fe)O, the iron content of atomic fraction 0.286 or more is obtained both by the almost entire substitution of Fe^{2+} ions of the (Ni, Zn, Fe) Fe_2O_4 solid solution by the Ni^{2+} ions (to a great extent) and by Zn^{2+} ions according to the reaction:

$$(Ni, Zn)_{1-x}\,Fe_{2+x}O_4 + x(Ni^{2+}, Zn^{2+}) = (Ni, Zn)\,Fe_2O_4 + xFe^{2+}.$$

At this phase boundary a part of Fe^{2+} ions probably oxidizes up to Fe^{3+} ions, and from the appearing Fe_2O_3 according to the reaction:

$$(Ni, Zn)_{1-x}\,Fe_{2+x}O_4 + \tfrac{3}{8}x(Ni^{2+}, Zn^{2+}) + \frac{x}{4}\,O_2 = \left(1 + \frac{x}{8}\right)(Ni, Zn)\,Fe_2O_4 + \tfrac{3}{4}xFe^{3+},$$

an additional quantity of the ferrite phase crystallizes.

It is quite possible that it is the run of the reaction that brings about a more dense ferrite layer at the boundary with (Ni, Zn, Fe)O than in other areas of this layer. In interacting NiO or (Ni, Zn)O with Fe_2O_3, according to the model of interdiffusion of ions Fe^{2+} and Ni^{2+}, Zn^{2+} ions, the equivalent volume of the reaction product is $1/2V_M$. In this case the Wagner–Schmalzried equation is as follows:

$$K_r = Z_c C_c \tilde{D}_c \cdot \frac{2\Delta G^0}{RT}$$

To determine which of the extreme cases of the interdiffusion process is, in fact, realized and the diffusion of which ions limits

the reaction rate, the rational constants of the interaction rates are calculated using for both cases the Wagner–Schmalzried equation. The obtained values are compared to those calculated by the formula $K_r = k/2V$ (experimentally determined constant), where k is the constant of the parabolic law of growth of the ferrite layer thickness and V is the equivalent volume.

The molar volumes of the (Ni, Zn)$_{1-x}$Fe$_{2+x}$O$_4$ ferrite phase, containing 0.31 atomic fraction of iron, are determined using the crystal lattice parameter, calculated according to the additivity law of the crystal lattice parameters of nickel, zinc, and magnetite ferrites. The free energy of formation for these compounds is calculated using the ΔG^0 values of magnetite and zinc nickel ferrites, taken from (*9*), assuming that they form an ideal solid solution. When the reaction rate is limited by the Ni^{2+}, Zn^{2+}, diffusion, the $\tilde{D}$ values of interdiffusion coefficients of the $NiFe_2O_4$–$ZnFe_2O_4$ system (*10*) are substituted into the Wagner–Schmalzried equation at total nickel and zinc concentration, which for the investigated ferrite layer with C_{Fe} = 0.31 atomic fraction is 0.12 atomic fraction. The iron diffusion coefficient values are taken from the curve of iron distribution in the ferrite phase also with C_{Fe} = 0.31 atomic fraction.

The comparison of the rational constant values of the investigated interaction rates obtained by the $K_r = k/2V$ formula with K_r values calculated by the Wagner–Schmalzried equation for two extreme mechanisms of interdiffusion shows that the interaction rate is limited by the Fe^{2+}, Fe^{3+} ion diffusion rather than by the diffusion of Ni^{2+}, Zn^{2+} (Fig. 7). At temperatures above 1265°C, the second extreme case of interdiffusion, related to the Fe^{2+} ion diffusion, is realized and below this temperature both Fe^{2+} ions and Fe^{3+} ions diffuse.

With zinc content growing in the initial (Ni, Zn)O solid solution the Fe^{3+} ion fraction increases in the interdiffusion process when compared to that of Fe^{2+} ions. The K_r values calculated taking into account the fact that the reaction rate is limited by the Fe^{3+} ion diffusion (Fig. 7) are located near the experimental K_r values (Fig. 7).

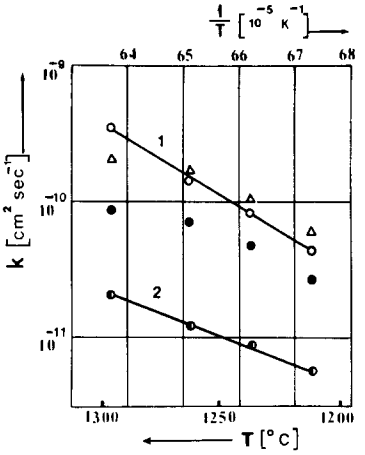

FIG. 7. Temperature dependence of ln K_r for the $Ni_{0.86}Zn_{0.14}O$–Fe_2O_3 system. The ln K_r values are determined using the experimental K_r (1) (○) and the interdiffusion coefficients Ni and Zn in the $NiFe_2O_4$–$ZnFe_2O_4$ system (2) (◐); (△), (●)—the K_r values calculated using the Wagner–Schmalzried equations in the case when the reaction rate is limited by the ion diffusion Fe^{2+} (△) and Fe^{3+} (●).

However, at 1215–1295°C in interacting (Ni, Zn)O with Fe_2O_3 in addition to the interdiffusion mechanism there operates a mechanism involving: zinc evaporation from the (Ni, Zn)O solid solution, its transport to the (Ni, Zn, Fe)O/ferrite interface through the gaseous phase, and further transport of Zn^{2+} and electrons or O^{2-} through the ferrite layer towards the ferrite/Fe_2O_3 boundary with subsequent formation of an additional ferrite layer at this boundary using the reactions:

$$Fe_2O_3 + (1-x)Zn^{2+} + 2(1-x)e^- + \frac{3-4x}{6}O_2 = \frac{3-x}{3}Zn_{3(1-x)/(3-x)}Fe_{2x/(3-x)}Fe_2O_4,$$

$$4\,Fe_2O_3 + Zn^{2+} + 2e^- = 3\,Zn_{1/3}Fe^{2+}_{2/3}Fe^{3+}_2O_4.$$

The contribution of this mechanism grows with zinc concentration in (Ni, Zn)O with it being dominant for zinc ferrite. Thus, the interaction of (Ni, Zn)O with Fe_2O_3 is realized by the mixed type mechanism, according to which both the cation interdiffusion of Fe^{2+}, Fe^{3+} and Ni^{2+}, Zn^{2+} and one-sided diffusion of Zn^{2+} and electrons or O^{2-} take place. The relation between these mechanisms depends on temperature and on the (Ni, Zn)O solid solution composition.

References

1. V. V. PAN'KOV AND L. A. BASHKIROV, *Izv. Akad. Nauk. BSSR Ser. Khim. Nauk* **N.2,** 49 (1976).
2. L. A. BASCHKIROV, P. KLEINERT, AND L. HEINKE, *Z. Anorg. Allgem. Chem.* **366**(1–2), 51 (1969).
3. G. ECONOMOS, *J. Amer. Ceram. Soc.* **42**(12), 628, (1959).
4. M. PAULUS AND P. V. EVENO, "Reactivity of Solids," p. 585. Wiley, New York, (1969).
5. D. CEVOVIC, I. MOMCILOVIC, S. J. KISS, AND S. MALCIC, "Reactivity of Solids," p. 774. Chapman & Hall, London (1972).
6. L. A. BASHKIROV, M. G. BASHKIROVA, *Izy. Akad. Nauk. SSSR Ser. Neorg. Mater.* **7,** 2218 (1971).
7. S. L. BLANK AND J. A. PASK, *J. Amer. Ceram. Soc.* **52,** 669 (1969).
8. H. SCHMALZRIED. *Z. Phys. Chem.* B **33,** 3 (1962).
9. YU. D. TRETYAKOV, "Termodinamika Ferritov." Khimiya, Leningrad (1967).
10. V. V. PAN'KOV, L. A. BASHKIROV, YU. G. SAKSONOV, AND G. YA. FEDOROVA, *Dokl. Akad. Nauk. SSSR* **233,** 1150 (1977).